

Photonic Crystals: Towards Ultrasmall Lightwave Circuits

Masaya Notomi[†], Akihiko Shinya, and Eiichi Kuramochi

Abstract

A photonic crystal having photonic band gaps is expected to play a key role in future large-scale photonic integrated circuits. We have been investigating two-dimensional silicon-on-insulator (SOI) photonic crystal slabs and have demonstrated that such a slab is a good candidate for the basic platform of photonic-crystal-based circuits. In this paper, we show how to design photonic crystals of this type to implement various components. As a result of appropriate design and with the help of advanced Si nanofabrication technology, we have successfully made various ultrasmall photonic-band-gap waveguides, resonators, and functional components in SOI photonic crystal slabs with operating wavelengths covering most of the fiber communication wavelengths.

1. Introduction

A *photonic crystal* is a structure whose refractive index is periodically modulated on the scale of an optical wavelength. Such a *crystal* is predicted to possess various unique characteristics that cannot be achieved in conventional materials. This is analogous to electronic properties in conventional materials. Various electronic properties—such as conducting, semiconducting, or insulating—arise from electrons in crystals feeling periodic perturbation from the lattices, resulting in the formation of so-called energy band structures. In a similar way, light propagation in photonic crystals (PhCs) can be largely controlled because photons in crystals feel periodic perturbation, resulting in the formation of photonic band structures. As **Fig. 1** shows, the dispersion relationship in conventional materials is fundamentally different from that in PhCs. The former usually exhibits a photonic band gap (PBG) in which there are no propagation modes. PhCs within this PBG frequency range behave as if they were photonic *insulators*, which do not exist in nature (for conventional materials). In addition, the curvature of the dispersion curve is also very different from that of conventional mate-

rials, which means that the traveling speed of light can be controlled over a wide range.

PhCs with PBGs are expected to be key platforms for future large-scale optical integrated circuits [1], [2]. Making optical (photonic) ICs or LSIs has been an important target of photonics technology since it started several decades ago, but it is still an engineer's dream. This is mostly due to the very fundamental characteristic of light: photons do not interact efficiently with materials or with other photons. This makes it difficult to confine photons in a tiny space and also leads to poor controllability. Most optical components rely on total internal reflection (TIR) to confine the light, but TIR becomes ineffective for small components. (This is because TIR is effective only for a certain range of propagation directions.) Actually, optical components are normally significantly larger than the optical wavelength. PhCs with PBGs give us another mechanism for confining light. Since the reflection caused by PBGs is effective for all angles, PBG confinement works even for wavelength-scale components. In PhCs, point defects function as optical cavities (PBG resonators) while line defects function as optical waveguides (PBG waveguides). The coupling of PBG resonators and waveguides leads to functional devices. Thus, putting a large number of various functional defects into PhCs with PBGs (equivalent to creating photonic insulating substrates) leads to photonic ICs/LSIs

[†] NTT Basic Research Laboratories
Atsugi-shi, 243-0198 Japan
E-mail: notomi@nttbl.jp

(Fig. 2). Since the size of each component is comparable to the optical wavelength, the total size of circuits will be significantly less than that of conventional optical circuits. In addition, the strong confinement of light in PBGs enhances the interaction

between light and matter, as in amplification and optical nonlinear switching, for example.

In this paper, we describe some design and measurement issues related to PBG waveguides and resonators in two-dimensional (2D) PhC slabs (mainly

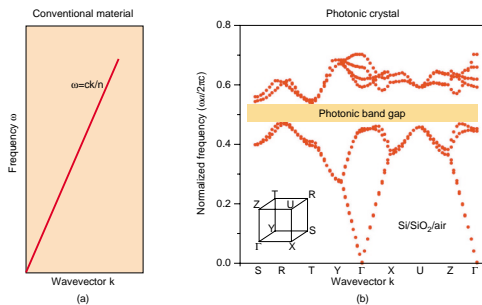


Fig. 1. Dispersion relationship of light in (a) conventional dielectrics and (b) typical photonic crystals. (a : the lattice constant)

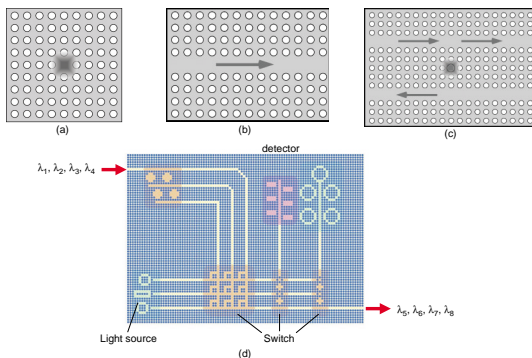


Fig. 2. Schematics of various components in PhCs. (a) Point defect in a PhC acting as a resonator, (b) line defect in a PhC acting as a waveguide, (c) coupled defects in a PhC acting as a functional component, and (d) schematic of a PhC-based circuit.

SOI PhC slabs). We show that ultrasmall waveguides and resonators having a small radiation loss can be made using available lithographic nano-fabrication techniques. Indeed, some of their unique properties have already been observed experimentally. In addition, we discuss various functional elements produced by coupling PBG waveguides and resonators. This final topic is very important for integrated-circuit applications.

2. Two-dimensional SOI photonic crystal slab

It might seem natural to choose 2D PhCs for photonic IC applications because the geometry of any conventional circuit is basically two-dimensional. Actually, most theoretical studies of PhC-based circuits assumed ideal 2D PhCs, that is, infinitely thick 2D crystals. However, such simple 2D crystals are not practical because light will leak out in the out-of-plane direction due to the lack of vertical confinement mechanisms. Of course, proper implementation of circuit elements within 3D PhCs having full PBGs should solve this problem, but such fabrication is very

challenging. Considering how easy it is to fabricate 2D PhCs, one key issue is how to introduce efficient vertical confinement in 2D PhCs. Recent studies have shown that it is indeed possible to achieve efficient vertical confinement within 2D PhCs by various methods. In this paper, we show that such efficient 2D PhCs can be made using silicon-on-insulator (SOI) substrates.

Figure 3 shows schematic figures of the fabrication process of SOI PhC slabs and electron micrographs of a bulk PhC and a waveguide within a PhC. Periodic hole patterns are formed on the top Si layer of an SOI substrate by electron beam lithography and electron-cyclotron-resonance ion stream dry etching [3]. This patterned Si layer acts as a 2D PhC. The SiO₂ layer works as a lower cladding layer, and the upper cladding layer is air. We refer to this structure as a SiO₂-clad PhC slab. Sometimes we selectively etch off the SiO₂ layer to form an air-bridge structure. In such cases, both cladding layers are air. We call this an air-clad type PhC slab. PhC slabs are 2D PhC structures located within high-index-contrast slab waveguides. In PhC slabs, light waves are confined

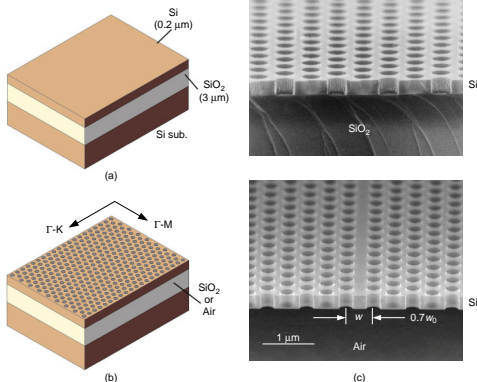


Fig. 3. Schematics of the fabrication process. (a) An SOI substrate on which PhCs are to be fabricated. (b) Periodic hole patterns formed by electron beam lithography and dry etching. (c) Electron micrographs of SOI PhC slab and a line-defect waveguide fabricated in a similar structure. The waveguide shown here is an example of width-varied waveguides (discussed in 3.2). ($w_0 = \sqrt{3}a$, where a is the lattice constant.)

by a combination of in-plane PBG confinement and vertical TIR confinement. Although we still use TIR in the vertical direction, light waves can be strongly confined within ultrasmall waveguides and resonators in PhC slabs without practical leakage if we design their structures appropriately.

So, how can we make meaningful 2D PBGs in these 2D PhC slabs? **Figure 4(a)** shows the photonic band structure of Si PhC slabs. The red lines in the graph show band dispersion calculated by the plane-wave expansion method, and gray lines are *light lines* of the cladding material (air and SiO₂). The *light line* is defined as $\omega = ck/n$, and modes above this light line of the cladding are leaky because they overlap with radiation modes in the cladding. PBGs below the light line can work as meaningful 2D PBG without radiation loss. If the refractive index n of the cladding material is not so small, the position of the light line

is lower, leading to a reduction or vanishing of the usable PBG region. In this sense, a large index contrast (between Si and SiO₂) in SOI substrates is advantageous for large 2D PBGs.

If we wish to construct PhC-based photonic ICs, we must first confirm whether appropriate PBGs are formed at desired wavelengths. We have directly measured the transmittance of 2D SOI hexagonal air-hole PhCs by using a single-mode tapered fiber and a wideband white light source. **Figure 4(b)** shows transmittance spectra along two crystal axes and the corresponding photonic band diagram for transverse electric wave (TE) polarization. We observed a common PBG from 1.23 to 1.58 μm for Γ -K and Γ -M crystal-axis orientations, which shows that a full PBG is open in the 2D plane. The experimental result agrees very well with the 3D finite-difference time-domain (FDTD) calculation [4], [5]. The observed PBG covers the entire wavelength range currently used for optical communications. Thus, this result shows that SOI photonic crystal slabs can be considered as possible platforms for photonic ICs in this wavelength range.

3. PBG waveguides

3.1 Design

Next, we examine how to make efficient waveguides in 2D PhC slabs. Our goal is to make a wideband single guiding mode that operates within the PBG. In fact, if we use only a straight isolated waveguide, then the position of the mode relative to the PBG is not a serious matter. However, if we want to make bends, splitters, or coupling to point-defect cavities (which is always the case with practical applications), then we need a PBG in the operating band. **Figure 5(a)** shows the calculated waveguide dispersion of typical line-defect waveguides in hexagonal PhC slabs. In Fig. 5(a), there are two modes within the PBG: an even mode and an odd mode. Thus, the single-mode bandwidth is limited by the existence of this second odd mode. In addition to the position of the PBG, we must consider the position of the light line of the cladding material. The TIR confinement in the vertical direction is lost in the mode above the light line, and the mode becomes leaky. It should be noted that theoretically the mode below the light line is a truly guided mode that has no propagation loss. We estimated the loss of the leaky modes just above the light line to be about 100 dB/mm [6], which we think is too large for most applications, although leaky modes can be used under certain limited condi-

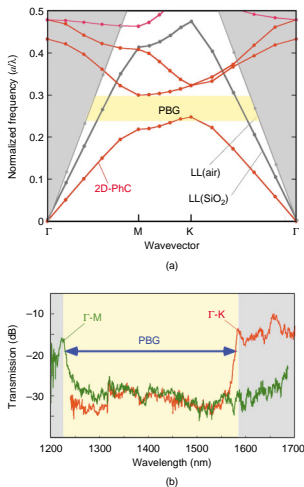


Fig. 4. Bulk properties of SOI PhC slabs. (a) Calculated photonic band structure of 2D SOI PhC slabs and (b) transmission spectra of SOI PhC slabs.

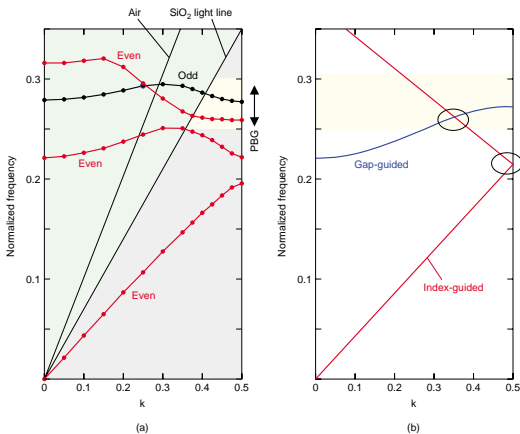


Fig. 5. Dispersion of PBG waveguides. (a) Theoretical dispersion curves of single-missing-hole line-defect waveguides in hexagonal PhC slabs and (b) intuitive understanding of the same mode as in (a).

tions.

Therefore, we must design a wideband single-mode condition *below the light line* within the PBG. Since a wide bandwidth requires a large slope of the dispersion curve in the limited wavevector space, a large group velocity is preferable. The previous section suggests that we can control the operating wavelength and group velocity of waveguiding modes by appropriately controlling the modes having different characteristics and also by controlling the so-called anticrossing behavior which we discuss below.

We have already examined this light-line problem in PhC slabs in detail [6], [7]. The following briefly summarizes the issue. In the case of air-clad PhC slab structures, a conventional single-missing-hole-line waveguide (Fig. 5(a)) has a relatively wide single-mode bandwidth. But with SiO₂ (or polymer) clad PhC slabs, the same single-missing-hole-line waveguide has only a very small bandwidth. This happens because a TIR-guided mode (with a negative curvature) and a PBG-guided mode (with a positive curvature) cross each other in the PBG under the light line

of SiO₂ in a normal single-missing-hole-line defect, and the anticrossing of two modes with opposite curvatures results in a very flat band, namely a very small width. The situation is graphically shown in Fig. 5(b). Since this anticrossing occurs accidentally in this position, we can change the situation by changing the geometrical structure of the defect.

To solve this problem, we introduced a new waveguide structure, namely *width-varied line-defect waveguide*. The left diagram of Fig. 6(a) shows a width-varied line-defect waveguide, in which the width W is varied from the normal width $w_0 (= \sqrt{3}a$, where a is the lattice constant). By reducing the width, we created another band with a large group velocity that enters the PBG from the lower band edge. We fabricated a width-reduced PBG waveguide on SOI PhC slabs and experimentally demonstrated that this modification produced a wideband transmission window for SiO₂-clad PhC slabs as shown in Figs. 6(b) and 6(c). We confirmed that this waveguide has a very small propagation loss (6 dB/mm), which is comparable to normal single-missing-hole-

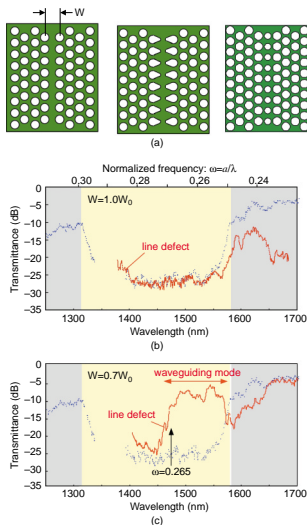


Fig. 6. Structural tuning of PBG waveguides. (a) Various examples of structural tuning (width-varied, egg-shaped-hole, and phase-shifted-hole) and (b) and (c) transmission spectra of PBG waveguides in 2D SOI PhC slabs with SiO_2 cladding, where the waveguides are normal single-missing-hole line defect waveguides in (b) and width-reduced line defect waveguides in (c). a is the lattice constant.

line defects in air-clad PhC slabs. In fact, a normal single-missing-hole-line defect has a relatively small truly single-mode condition. Thus, the width-reduced waveguide also improves the width of the truly single-mode condition even for air-clad PhC slabs.

Width reduction is not the only way to solve the problem for SiO_2 -clad PhC slabs. Because PBG waveguides have a large degree of freedom when the dispersion is tuned, there are many other ways to achieve this in an equally practical manner. Examples of other tuning methods are shown in Fig. 6(a) [7]–[9].

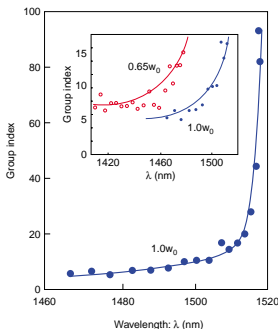


Fig. 7. Group velocity dispersion measurement. Measured group index as a function of wavelength.

3.2 Group velocity dispersion measurement

As discussed in the previous section, the dispersion can be tuned over a wide range in PBG waveguides, which is one of their most important features. A large dispersion over a wide wavelength range, as seen in Fig. 5(a), cannot be achieved by other conventional dielectric waveguides. In addition to simple applications to dispersion-controlled waveguides, such a large dispersion and good controllability of group velocity may prove important for various applications related to optical nonlinear phenomena. In terms of physics, it is well known that light-matter interaction in materials is strongly influenced by the group velocity of light.

Here, we describe our experimental study of the group velocity dispersion of PBG waveguides in SOI PhC slabs [10]. Since there is some reflection at both ends of our PBG waveguides, we can observe a Fabry-Perot interference pattern in the transmission spectra. This interference pattern is directly related to the group index of the waveguide, so we can deduce the group index if we know the precise length of the waveguide. **Figure 7** shows the deduced group index of two different PBG waveguides: a normal single-missing-hole-line waveguide ($W=1.0w_0$) and a width-reduced waveguide ($W=0.65w_0$). The deduced group index shows an extremely large group velocity dispersion. It also shows an extremely large group

index that reaches almost 100 in the vicinity of the mode gap.

This large group index value means that the group velocity in this waveguide is very small. Recently, slow light modes in materials have been observed in various phenomena including electromagnetically induced transparency [11] and coherent population modulation [12], by controlling the *material dispersion*. Such slow modes are expected to provide ultimate control of the light-matter interaction with a very small light intensity. The origin of the slow light modes in Fig. 7 is very different (it is purely due to control of the *structural dispersion*), but this result indicates that a PBG waveguide may be another candidate for enhancing light-matter interaction.

3.3 Coupling to fibers

One of the most frequently addressed problems concerning PBG waveguides is their poor coupling efficiency with conventional single-mode fibers. This is a fundamental problem because the mode size for line-defect waveguides is always very much smaller than that for silica single-mode fibers. This smallness is usually considered to be an advantage for PhCs, but it is a fatal disadvantage for coupling. The typical cross-sectional size of a PBG waveguide is $0.4 \times 0.2 \mu\text{m}^2$, which is approximately three orders of magnitude smaller than that of a silica single-mode fiber. Moreover, there is a large reflection loss due to the large index difference between PBG waveguides and

silica fibers.

To solve this problem, we designed an adiabatic mode connector, which is monolithically integrated in an SOI PhC slab chip [13]. As schematically shown in Fig. 8, the connector consists of two parts: i) a spot-size converter (SSC), which adiabatically connects a polymer single-mode waveguide, a Si-wire waveguide, which was invented by NTT Microsystem Integration Laboratories [14], and a mode-profile converter (MPC), which adiabatically connects a Si-wire waveguide and ii) a photonic-crystal waveguide. The mode size and the refractive index of the polymer waveguide were designed to be the same as those of a high- Δ single-mode fiber. The mode size in the Si-wire waveguide was designed to be the same as that in the PBG waveguide. The fabrication process is very simple, namely a combination of a single-stage Si etching process and a conventional polymer waveguide process.

We fabricated this device and investigated its connection loss. The measured connection loss was 3–4 dB per port, which is the sum of the connection losses for SSC and MPC. Compared with the value of 30 dB, we significantly reduced the connection loss. Recently, a connection loss of 0.8 dB per port in an SSC for Si-wire waveguides was reported by NTT Microsystem Integration Laboratories [14]. If we combine that with this technology, we believe that we can further reduce the connection loss for PBG waveguides.

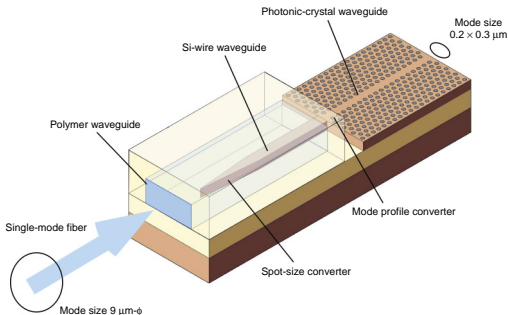


Fig. 8. Adiabatic mode connector containing a spot-size converter and a mode-profile converter.

4. PBG resonators

4.1 Design

With conventional optical resonators, which rely on TIR confinement, their quality factor (Q) is limited by their mode volume. That is, if the mode volume is reduced to a wavelength-scale size, Q will always decrease to a very small value. This can be intuitively explained as follows. Small-volume modes have a broad distribution in k -space, but TIR confinement only works for the k component that satisfies the TIR condition. That is, a broad k distribution results in a decrease in Q . However, PBG confinement does not impose such a restriction on the k distribution. Therefore, ultimately small-volume and high- Q resonators are expected to be achieved by PBG resonators. Such small and high- Q resonators are required for large cavity quantum electrodynamics (cavity-QED) effects in the solid state and are also important for various applications, such as lasers, emitters, and switching devices. This is the most important feature of PBG resonators.

In this context, a 3D PBG seems to be a fundamental requirement because 2D PBG resonators impose a similar restriction on the k distribution in the out-of-plane direction. In fact, the Q of 2D PBG resonators decreases when the mode size is reduced. It is not easy to make high- Q resonators in 3D-PBG materials because a high Q requires very high homogeneity in a relatively large volume. Recently, however, there has been considerable success regarding this matter in 2D PhC slabs. Several strategies have been proposed for increasing the Q value of wavelength-scale resonators in 2D PhC slabs. They are all intended to minimize the k distribution inside the radiation cone of the 2D PhC slabs (which is simply the light cone of the cladding material discussed in 2.2.) It has been numerically shown that modifications to the symmetry of cavity modes can lead to a fundamental increase in the Q of 2D PBG resonators. Johnson et al. [15] proposed using multi-nodal modes in a square lattice in which the radiation in the vertical direction is reduced by destructive interference. Ryu et al. extended their idea [16] and used whispering gallery modes (quadrupole modes) in square PhC slabs. Vuckovic et al. [17] showed that the introduction of edge dislocations in the center of the dipole modes in hexagonal PhC slabs increased Q .

We investigated multi-nodal modes in hexagonal PhC slabs. High- Q resonators in hexagonal PhCs are very important because they have the largest 2D PBG [18]. First, we must look for suitable multi-nodal

modes in hexagonal PhC slabs. Many kinds of multi-nodal modes can be obtained in a large cavity, but we want to keep the volume as small as possible. The smallest volume mode is known to be a dipole mode in a single point defect cavity [19], which is not favorable in terms of achieving a high Q value, so suitable multi-nodal modes should have a slightly larger volume than a dipole mode and a significantly larger Q value. It is well known that PBG cavities in hexagonal PhCs can have multi-nodal modes whose angular momentum numbers are $M=1, 2, 4, 6, 12$, etc. Of these, the most suitable candidate is the hexapole mode because it is the smallest order of multi-nodal modes whose symmetry matches the symmetry of the crystal lattice. To eliminate the vertical radiation loss, a very delicate balance is required. Thus, other modes, such as quadrupole modes, are inferior in terms of obtaining a small volume and a large Q .

In Fig. 9, we plot our design of hexapole mode cavities (a) and the electric field distribution of a typical hexapole mode in real space (b) and k -space (c and d). The real image clearly shows the three-fold rotational symmetry of this mode. The k -space distribution shows that the Fourier intensity is largely concentrated around six M points (one of the symmetry points in the reciprocal space for hexagonal lattices). The white circles in (c) and (d) represent the light cones of air. There is almost no intensity inside the light cones. This clearly shows that this mode exhibits very little radiation into the air. Figure 9(e) shows Q and V as a function of the resonance frequency (the varied parameter is r_m). Here the hole radius r of the crystal is kept constant at $0.35a$. A significantly high Q value of 5×10^5 is obtained when $r_m=0.26a$. The effective mode volume V is $0.9(\lambda/n)^3$, which is slightly larger than that of the dipole modes in hexagonal PhCs but still a very small value. It should be noted that when Q is at its maximum value, V is almost at its minimum in this case. The high Q and small V mechanisms must be similar to those in the quadrupole modes in square PhCs. These values (higher Q and smaller V) in hexagonal PhCs compared with those in square PhCs can be attributed to the larger PBG bandwidth of the hexagonal PhCs and the larger azimuthal mode number ($=3$) of the hexapole modes. The achieved Q is already much larger than those of other high- Q cavities in PhC slabs. But we found that further improvement was possible by varying the radius of the crystal. When $r=0.275a$, a Q of 2×10^6 was achieved at $r_m=0.26a$. In this condition, the resonance frequency approached the band edge, so mode delocalization also contributed to improving

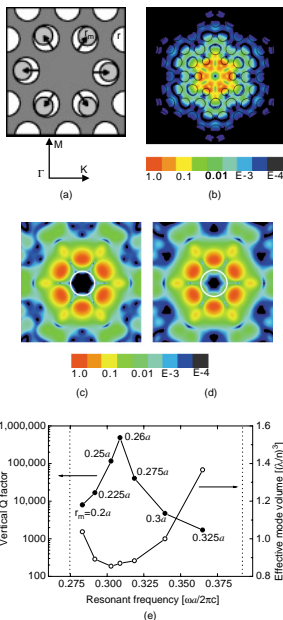


Fig. 9. High-Q PBG resonator: (a) hexapole single-defect PBG resonator in hexagonal PhC slabs, (b) electric-field distribution in real space, (c) and (d) electric-field distribution in Fourier space, where $r_m=0.26a$ and $Q=480,000$ in (c) and $r_m=0.30a$ and $Q=11,000$ in (d), and (e) calculated Q and mode volume (V) of hexapole modes as a function of the resonance frequency.

the Q value.

4.2 Coupling between PBG resonators and waveguides

Isolated resonators themselves may be useful for laser or light emitting device applications, but res-

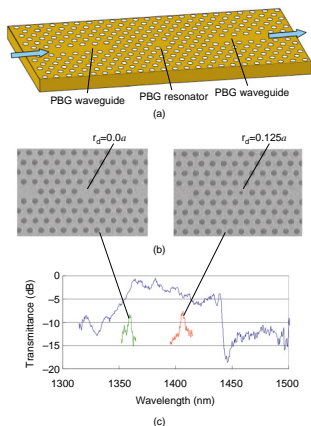


Fig. 10. Resonant tunneling filter. (a) Schematic view, (b) scanning electron micrographs of the devices, and (c) transmission spectra.

onators coupled to other optical elements (waveguides or other resonators) [20], [21] are more important because these coupled elements will be key components in future PhC-based optical circuits. Here we investigate an example of such a coupled element, as shown in Fig. 10(a). In this device, a single resonator is coupled to two straight waveguides (input and output). Light from the input waveguide can pass through the resonator into the output waveguide by resonant tunneling. This tunneling occurs only when the light wavelength matches the resonance wavelength of the cavity. That is, this device works as a wavelength filter. We call this a (two-port) resonant tunneling filter [22].

Figure 10(b) shows scanning electron micrographs of resonant tunneling filters fabricated in SOI PhC slabs with air cladding, where a single point-defect cavity was placed between two line-defect waveguides in hexagonal PhC slabs. The measurement results are shown in Fig. 10(c). We observed sharply resonant transmission within the transmission window of the PBG waveguides. It is important to note

that the resonant transmission wavelength changed as we changed the hole radius of the point defect. In this way, this device functioned as a wavelength-tunable narrow-band transmission filter. The resonant wavelength can be easily tuned by modifying the geometrical shape of the point defects.

The performance of this device is represented by the transmission Q and transmission intensity. The transmission characteristics of these resonance devices can be analyzed using the coupled-mode theory [23]. This analysis confirmed that the transmission characteristics can be explained by vertical Q (Q_V) and horizontal (in-plane) Q (Q_H). The Q_V is mainly due to decay into the radiation loss from the cavity, that is, the Q of the isolated cavity, if the crystal size is sufficiently large. Q_H is mainly due to decay into the waveguides as a result of coupling. Thus, the total Q (Q_T) is given by $1/Q_T = 1/Q_V + 1/Q_H$, and energy transmittance (T) is expressed as $T = (Q_T/Q_H)^2$. Thus, to achieve a high Q_T and a high T simultaneously, we must carefully design Q_V and Q_H to achieve optimization. The transmittance was very low (a few percent) in the result shown in Fig. 9(c), because Q_H is too high compared with Q_V .

With this in mind, we designed another resonant tunneling filter, as shown in Fig. 11(a). The basic

structure consists of a width-reduced ($W=0.65w_0$) waveguide, but the radius of the nearest-neighbor holes was slightly varied in the barrier region (this part is equivalent to a $0.40w_0$ waveguide). Since the mode gap of $0.40w_0$ waveguides is located within the transmission window of $0.60w_0$ waveguides, the light field is confined in this mode gap wavelength region. That is, the center part (cavity part) functions as a resonator although there is no true PBG in the barrier part. This design has two advantages. One is that it is easy to change Q_H continuously by changing the width of the barrier part. This continuous tunability of Q_H is effective in achieving a high transmittance. Another advantage is that this device can work with SiO_2 cladding and also adiabatic mode connectors. This is not the case for the structure shown in Fig. 10(a), where $1.0w_0$ PBG waveguides are used. It should also be noted that the adiabatic mode connector does not fit PhC slabs with air cladding.

We fabricated this type of resonant tunneling filter with adiabatic mode connectors as described previously. The adiabatic mode connectors were fabricated using the same process as before. This is the first PBG resonator device that can be directly connected to single-mode fibers. Figure 11 shows the transmission spectra of this device. The measured Q and ener-

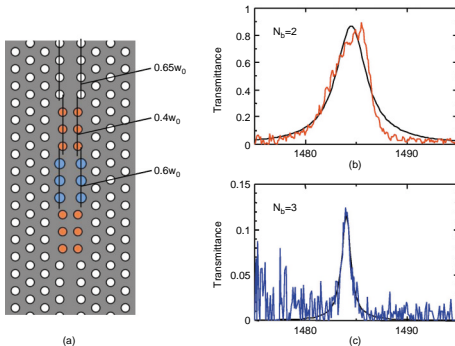


Fig. 11. Mode-gap resonant tunneling filter with adiabatic mode connector. (a) Schematic view and (b) and (c) experimental transmission spectra for two values of N_b (number of holes for the $0.4w_0$ waveguide section, i.e., the barrier thickness). Solid lines are Lorentzian-fitted curves.

gy transmittance values were 408 and 86% for (b) and 1350 and 12% for (c), respectively. N_b is the barrier thickness, that is, the number of holes for the $0.4w_0$ waveguide section. We achieved a significant improvement in the transmittance compared with the result in Fig. 10(c).

Further improvement of this filter requires an improvement in Q_H , which means that we must combine high-Q PBG cavities with PBG waveguides with an appropriate coupling strength. We recently improved these resonant tunneling filters [24]. Instead of single-missing-hole point defects, we used two-point defects to achieve high Q_V . As a result of tuning the size of nearest-neighbor holes, we obtained Q_V as high as 28,500. By appropriately designing the barrier between resonators and waveguides (that is, adjusting Q_H), we achieved $Q_T=7000$ and $T>70\%$ simultaneously.

In this section, our discussion was limited to two-port devices, but future studies should investigate more complicated resonator-waveguide coupled devices, such as devices with four or more ports.

5. Summary

Future PhC-based photonic integrated circuits will be based on a combination of PBG waveguides and PBG resonators. In this paper, we investigated various PBG waveguides and resonators in 2D PhC slabs, especially 2D SOI PhC slabs, which can be made on commercially available SOI substrates using existing mature Si nano-fabrication technology. Thus, 2D PhC slabs have a great advantage over other forms of PhC, but there is a severe limitation to 2D PhCs because they have a PBG only in the in-plane direction. In this study, we showed how this limitation affects the performance of PBG waveguides and resonators and demonstrated how we can design waveguides and resonators to overcome this limitation.

With appropriate design, it is possible to achieve efficient PBG waveguides in PhC slabs that include air and SiO_2 cladding. We fabricated various types of PBG waveguide in SOI PhC slabs. An extremely large group dispersion, which is one of the most interesting features of PBG waveguides, was experimentally confirmed for the fabricated waveguides. We made PBG waveguides with adiabatic mode connectors, which greatly improved the connection efficiency between PBG waveguides and single-mode fibers.

The effect of incomplete PBGs in PhC slabs is more severe for PBG resonators. However, we can also overcome this problem by using an appropriate

design. We used 3D FDTD simulation to show that ultrahigh-Q and small-volume resonators can be made in hexagonal PhC slabs. Finally, we investigated one of the simplest forms of resonator-waveguide coupled devices in PhC slabs, namely resonant tunneling filters. We fabricated resonant tunneling filters in SOI PhC slabs and studied how to design high-Q and high-transmittance devices. We made resonant tunneling mode-gap filters with adiabatic mode connectors and demonstrated that relatively high-Q and high-transmittance filters can be made.

These studies show that PBG waveguides and resonators in 2D PhC slabs have various promising features that overcome the fundamental limitations of 2D PhCs. We believe that the future direction of PhC-based photonic integration lies in the direction described in this paper. More complicated coupled devices and components will be studied in the future within a similar context.

References

- [1] E. Yablonovitch, "Inhibited spontaneous emission in solid-state physics and electronics," *Phys. Rev. Lett.*, Vol. 58, pp. 2059-2062, 1987.
- [2] J. D. Joannopoulos, R. D. Meade, and J. N. Winn, "Photonic Crystals," Princeton University Press, 1995.
- [3] C. Takahashi, J. Takahashi, M. Notomi, and I. Yokohama, "Accurate dry etching with fluorinated gas for two-dimensional Si photonic crystals," *MRS Proceedings* Vol. 637, E1.8, 2000.
- [4] I. Yokohama, M. Notomi, A. Shinya, C. Takahashi, and T. Tamamura, OEC, Makuhari, Chiba, Jul. 2000.
- [5] A. Shinya, M. Notomi, I. Yokohama, C. Takahashi, J. Takahashi, and T. Tamamura, "Two-dimensional Si-photonic crystals on oxide using SOI substrate," *Optical and Quantum Electronics*, Vol. 34, No. 1-3, pp. 113-121, 2002.
- [6] M. Notomi, A. Shinya, K. Yamada, J. Takahashi, C. Takahashi, and I. Yokohama, "Single-mode transmission within the photonic bandgap of width-varied single-line-defect photonic crystal waveguides on SOI substrates," *Electron. Lett.*, Vol.37, pp.243-244, 2001.
- [7] M. Notomi, A. Shinya, K. Yamada, J. Takahashi, C. Takahashi, and I. Yokohama, "Structural tuning of guiding modes of line-defect waveguides of SOI photonic crystal slabs," *IEEE J. Quantum Electron.*, Vol. 38, No. 7, pp. 736-742, 2002.
- [8] A. Shinya, M. Notomi, K. Yamada, C. Takahashi, J. Takahashi, and I. Yokohama, "Two-dimensional Si-photonic crystal single mode waveguide on SiO_2 substrate which functions above the light line," *OSA Topical Meeting of Integrated Photonic Research (IPR 2001)*, IMD4, Monterey, U.S.A., Jun. 2001.
- [9] A. Shinya, M. Notomi, and E. Kuramochi, "Single-mode Transmission in Commensurate Width-Variied Line-Defect SOI Photonic Crystal Waveguides," *SPIE Photonics West, Optoelectronics 2003*, San Jose, U.S.A., Jan. 2003.
- [10] M. Notomi, K. Yamada, A. Shinya, J. Takahashi, C. Takahashi, and I. Yokohama, "Extremely large group velocity dispersion of line-defect waveguides in photonic crystal slabs," *Phys. Rev. Lett.*, Vol. 87, 253902, 2001.
- [11] L. V. Hau, S. E. Harris, Z. Dutton, and C. H. Behroozi, *Nature*, "Light speed reduction to 17 metres per second in an ultracold atomic gas," Vol. 397, pp. 594-596, 1999.
- [12] M. S. Bigelow, N. N. Lepeshkin, and R. W. Boyd, "Observation of ultraslow light propagation in a ruby crystal at room temperature,"

Phys. Rev. Lett., Vol. 90, 113903, 2003.

- [13] A. Shinya, M. Notomi, E. Kuramochi, T. Shoji, T. Watanabe, T. Tsuchizawa, K. Yamada, and H. Morita, "Functional Components in SOI Photonic Crystal Slabs," *SPIE Proc. Vol. 5000*, 21, pp. 104-117, 2003.
- [14] T. Shoji, T. Tsuchizawa, T. Watanabe, K. Yamada, and H. Morita, "Low loss mode size converter from $0.3 \mu\text{m}^2$ square Si wire waveguides to single mode fibers," *Electron. Lett.*, Vol. 38, pp. 1669-1670, 2002.
- [15] S. G. Johnson, A. Mekis, S. Fan, and J. D. Joannopoulos, "Multipole-cancellation mechanism for high-Q cavities in the absence of a complete photonic band gap," *Appl. Phys. Lett.*, Vol. 78, pp. 3388-3390, 2001.
- [16] H.-Y. Ryu, S.-H. Kim, H.-G. Park, J.-K. Hwang, Y.-H. Lee, and J.-S. Kim, "Square-lattice photonic band-gap single-cell laser operating in the lowest-order whispering gallery mode," *Appl. Phys. Lett.*, Vol. 80, pp. 3883-3885, 2002.
- [17] J. Vuckovic, M. Loncar, H. Mabuchi, and A. Scherer, "Optimization of the Q factor in photonic crystal microcavities," *IEEE J. Quantum Electron.*, Vol. 38, No. 7, pp. 850-856, 2002.
- [18] H.-Y. Ryu, M. Notomi, Y.-H. Lee, "High quality factor and small volume hexapole modes in photonic crystal nanocavities," *Appl. Phys. Lett.*, Vol. 83, No. 21, pp. 4294-4296, 2003.
- [19] R. Coccioli, M. Boroditsky, K. W. Kim, Y. Rahmat-Samii, and E. Yablonovitch, "Smallest possible electromagnetic mode volume in a dielectric cavity," *IEEE Proc. Optoelectron.*, Vol. 145, No. 06, pp. 391-397, 1998.
- [20] S. Fan, P. R. Villeneuve, J. D. Joannopoulos, and H. A. Haus, "Channel drop tunneling through localized states," *Phys. Rev. Lett.*, Vol. 80, pp. 960-963, 1998.
- [21] S. Noda, A. Chutinan, and M. Imada, "Trapping and emission of photons by a single defect in a photonic bandgap structure," *Nature*, Vol. 407, pp. 608-611, 2000.
- [22] M. Notomi, "Photonic-band-gap waveguides and resonators," *LEOS 2003*, Tucson, Arizona, U.S.A., pp. 212-213, Oct. 2003.
- [23] C. Manoloutou, M. J. Khan, S. Fan, P. R. Villeneuve, H. A. Haus, and J. D. Joannopoulos, "Coupling of modes analysis of resonant channel add-drop filters," *IEEE J. Quantum Electron.*, Vol. 35, No. 9, pp. 1322-1331, 1999.
- [24] S. Mitugi, A. Shinya, E. Kuramochi, M. Notomi, T. Tsuchizawa, and T. Watanabe, "Resonant tunneling wavelength filters with high Q and high transmittance based on photonic crystal slabs," *LEOS 2003*, Tucson, Arizona, U.S.A., pp. 214-215, Oct. 2003.



Masaya Notomi

Distinguished Technical Member, Senior Research Scientist, Supervisor, Physical Science Laboratory, NTT Basic Research Laboratories.

He received the B.E., M.E., and Dr. Eng. degrees in applied physics from the University of Tokyo, Tokyo in 1986, 1988, and 1997, respectively. In 1988, he joined NTT Optoelectronics Laboratories. Since then, his research interest has been to control the optical properties of materials and devices by using artificial nanostructures, and he has been researching semiconductor quantum wires/dots and photonic crystal structures. In 1996-1997, he was at Linköping University, Sweden as a visiting researcher. Since 2002, he has also been a guest associate professor of Tokyo Institute of Technology, Japan. He is a member of the Japan Society of Applied Physics (JSAP) and the American Physical Society.



Akihiko Shinya

Physical Science Laboratory, NTT Basic Research Laboratories.

He received the B.E., M.E., and Dr. Eng. degrees in electrical engineering from Tokushima University, Tokushima in 1994, 1996, and 1999, respectively. In 1999, he joined the NTT Basic Research Laboratories. He has been engaged in R&D of photonic crystal devices. He is a member of JSAP.



Eiichi Kuramochi

Research Scientist, Physical Science Laboratory, NTT Basic Research Laboratories.

He received the B.E. and M.E. degrees in electrical engineering from Waseda University, Tokyo in 1989 and 1991, respectively. In 1991, he joined NTT Optoelectronics Laboratories, where he engaged in research on semiconductor nanostructures for photonic devices. He is currently researching photonic crystals. He is a member of JSAP.